Optics and Laser Technology 93 (2017) 208–215

Contents lists available at ScienceDirect

Optics and Laser Technology

journal homepage: www.elsevier.com/locate/jolt

Full length article

Fatigue behavior of superferritic stainless steel laser shock treated without protective coating

L. Spadaro [a], G. Gomez-Rosas [b], C. Rubio-González [c], R. Bolmaro [a], A. Chavez-Chavez [b], S. Hereñú [a,*]

[a] Instituto de Física Rosario-CONICET, Rosario, Argentina
[b] Departamento de Física, CUCEI, Universidad de Guadalajara, Guadalajara, Jal, Mexico
[c] Centro de ingeniería y desarrollo industrial, Querétaro, Mexico

ARTICLE INFO

Article history:
Received 30 November 2016
Received in revised form 1 February 2017
Accepted 5 March 2017

Keywords:
Superferritic stainless steel
Laser shock peening
Fatigue
Microstructure

ABSTRACT

The laser shock peening (LSP) is a new technique that improves the fatigue life of metallic components by inducing deep compressive residual stresses through the surface. However, the beneficial effects of LSP depend on the persistence and stability of such residual stress fields under cyclic loading and temperature. Moreover, if no absorbent coating is used in LSP operation, thermal effects can occur on the metallic substrate. The purpose of this work is to study the influence of LSP, without protective coating and with different pulse densities, on the low cyclic fatigue behavior of a superferritic stainless steel UNS S 44600. These results are correlated with observations performed by means of transmission electron microscopy (TEM) and scanning electron microscopy (SEM) with electron diffraction spectroscopy (EDS). The hole-drilling method is used to measure residual stresses. The micro-hardness and roughness profiles are also presented. This paper shows that LSP without coating produces beneficial compression residual stresses. However, in the first 10 μm beneath the surface, thermal effects occur that induce intergranular corrosion. This intergranular corrosion deteriorates the fatigue properties of a superferritic stainless steel UNS S 44600.

© 2017 Elsevier Ltd. All rights reserved.

1. Introduction

In order to improve the material properties, surface engineering is recommended, since without changing the bulk properties of a material their surface properties can be enhanced, allowing the use of a cheaper material. In this sense, two kinds of surface treatments can be done: heat treatments (nitriding, cementation) [1–4] and mechanical treatments (deep rolling, shot peening, or the current laser shock peening) [5–9]. All the mechanical surface treatments produce roughness, increase dislocation density and induce compressive residual stresses. The compressive residual stresses that are produced on the surface through different mechanical methods have shown to delay the fatigue crack nucleation as well as its propagation in different metals [7]. Since 1960 the possibility of generating shock waves by using pulsed lasers began to be studied. These shock waves cause permanent plastic deformation in metals generating compressive residual stress. This new technique is known as laser shock processing or laser shock peening (LSP) and it has wide applications in the manufacturing industry of engines, boats, cars and planes [7–9]. To generate shock waves of high amplitude, so as to plastically deform metals and generate compressive residual stress fields, laser pulses of high intensity and short duration are required. Nowadays, the lasers that meet these requirements are solid state lasers, which incorporate a Q-switch device that allows pulses in the nanosecond range. Thus, it is possible to achieve peak powers of GW. This high energy laser beam vaporizes the material and the vapour rapidly reaches temperatures above several tens of thousands degrees, whereupon the electrons are ionized from the atoms and the vapour is transformed into plasma. During this process, the plasma expansion generates a pressure wave that spreads into the material. Due to the high temperature the plasma reaches on the surface, heat propagation also occurs leading, depending on the alloy, to the ablation and fusion of 1–100 μm. Some authors recommend the use [8–11] of an absorbent coating (usually black paint) on the metal surface to protect it from thermal effects that can occur during the process. However, the parts to be peened are not always accessible to apply an ablative overlay or its use in an industrial configuration is expensive. Hence, a lot of research has driven to study laser peening without protective coating (LSPwC) [12,13]. In literature, the effects of LSPwC are referred to just a few stainless steel grades [14–17]. Additionally, in order to avoid that the plasma rapidly expands from the surface and thereby so as to increase the shock

* Corresponding author.
E-mail address: herenu@ifir-conicet.gov.ar (S. Hereñú).

http://dx.doi.org/10.1016/j.optlastec.2017.03.003
0030-3992/© 2017 Elsevier Ltd. All rights reserved.

wave intensity, a transparent overlay to radiation (confining medium) is also placed in the material surface. Water is the most commonly used coating for its versatility and availability [8,9].

The LSP processes have emerged as an effective alternative to the traditional processes to improve the fatigue properties in metallic materials. However, the magnitude of these beneficial effects depends on the microstructural changes produced by LSP in each alloy [17–20] and the degree of relaxation of the compressive stresses during cycling [21–23]. As regards stainless steels, scarce attempts have been developed to assess the LSP capability to enhance the low cycle fatigue properties [23]. Most researches deal with the beneficial effects of LSP on the high cycle fatigue regime (HCF), mainly in austenitic stainless steels [16,23–25].

Recently, significant research has been devoted to the development of cost-efficient stainless steels containing low Ni and Mo content. Thus, superferritic stainless steels, with lower cost alloying elements, has found increasing applications in many industries [26].

Therefore, the purpose of this research is to analyze the influence of LSPwC on the low cycle fatigue (LCF) behavior of a superferritic stainless steel. Special interest is placed on relating the cyclic behavior with the microstructure in order to discern the limit of cyclic deformation where LSP is effective.

2. Material and experimental procedure

The studied material is a superferritic stainless steel UNS S 44600 with the chemical composition (wt.%): C: 0.058; Cr: 23.58; Ni: 0.33; Mo: 0.13; Mn: 0.65; Si: 0.4; Cu: 0.15; V: 0.13; P: 0.02; N: 0.098, Nb: 0.09. This steel was received in the form of hot rolled square bar of 50.8 mm × 101.6 mm × 500 mm. From the bar, plates of 80 mm × 40 mm × 5 mm were cut in the rolling direction. The plate surfaces were polished with different grade SiC papers (from 60 to 320 grit) to eliminate the manufacturing effect of the original plates. These samples which received no further treatment are referred to as received (AR).

The LSP treatment were performed with a Q switched Nd:YAG laser operating at 10 Hz with a wave length of 1064 nm, energy of 1 J/pulse and the FWHM of the pulses was 6 ns. The spot diameter was 1.5 mm and the power density is held at a constant value of 9.4 GW/cm^2. A special device has been implemented to produce a controlled water jet that forms a thin water layer on the sample to be treated. Specimen treated area was 20 mm × 20 mm on both sides of the plates. No protective coating was used during LSP. A 2D motion system was used to control specimen position and generate the pulse swept. Controlling the velocity of the system, the desired pulse density was obtained.

Table 1 presents the variations in the LSP conditions employed in this work.

Through ASTM standard E837-1 [27] the residual stress distribution was measured by the hole-drilling method. Strain gage rosettes CEA-06-062UL-120 were used. Microhardness measurements were carried out in Shimadzu HMV-2 Vickers microhardness tester. The Vickers indentations were performed with loads of 245.2 mN during 10 s. The surface roughness of the steel with and without LSP was measured using a profilometer (Mahr Pocket Surf, Germany) with roughness filter cut off wavelength of 0.25 mm over the range of 1.75 mm. For each condition, the average roughness (R_a) was measured.

Table 1
LSPwC conditions.

Specimen	Overlap percentages (%)	Peening duration /cm^2 (minutes/cm^2)
1600 pulses/cm^2	79	2.66
2500 pulses/cm^2	83	4.16
5000 pulses/cm^2	88	8.33

From the plates with and without LSP, flat specimens for low cycle fatigue (LCF) were machined by electro-erosion. Fig. 1 shows the geometry of the fatigue specimens with the coverage area as well as the swept direction of LSP. LCF tests were conducted at room temperature under fully reversed plastic strain control, with plastic strain ranges of $\Delta\varepsilon_p = 0.1\%$ and $\Delta\varepsilon_p = 0.3\%$. In this study, the nomenclature of 'Peak Tensile Stress' is referred to the maximum stress (σ_{max}) in each cycle.

Specimens for optical metallographic observation were polished with diamond paste and electrolytically etched in 50% nitric acid in water solution at room temperature. Scanning electron microscopy (SEM) equipped with an energy dispersive spectroscopy (EDS) device was used. In order to observe the nearer dislocations structures to the surface in a transmission electron microscope (TEM), for the preparation of thin foils the following steps were followed: (i) At a depth of 1 mm from the surface, slices were cut; (ii) From the opposite side of the surface an initial thinning of the material until slices of 100 μm of thickness were obtained, was performed; (iii) 1 mm diameter discs were cut with a precision punch; (iv) The central regions of both sides of the discs were finally thinned with a double jet in a solution of 10% perchloric acid in ethanol. Therefore, the dislocations structures observed in this work represent the dislocations structures from the surface till approximately 100 μm.

3. Results and discussion

3.1. Near surface microstructure

Fig. 2 shows the optical micrographs obtained from the surface of UNS S44600 without and with LSP. Equiaxed grains are the characteristic microstructural feature in both AR and laser treated samples. Moreover, from this figure it is worthwhile to note that no evidence of discernible changes in grain size occurs by LSP. So as to corroborate this statement, the intercept method was used to determine the grain size. It was confirmed that no grain refinement was produced by LSP. In this sense, the AR and LSP treated specimens have an average grain size of 45 μm. Consistent with previous works [13,16], it seems that a single LSP impact causes no effect in grain size. On the other hand, grain refinement after multiple LSP impacts is reported in literature [9,28].

Whereas an electrochemical etching is needed to reveal the grain boundary in the steel without LSP, Fig. 2(a), the LSP without protective coating severely delineates the grains boundaries without any chemical attack, Fig. 2(b). This phenomenon is independently of the pulse density applied. Although LSP is actually considered as a mechanical surface treatment, thermal effects caused by the laser irradiation are unavoidable if the process is carried out without an ablative layers (LSPwC) [8,11,16]. Fig. 3 shows that through the observation of the cross section of the treated steel the depth of intergranular attack caused by the LSPwC reaches about 10 μm. In order to get further information to rationalize these results, constituent element distribution along the grain boundary was obtained by EDS (Fig. 4). In the material without LSP, Fig. 4(a), the chemical composition remains unchanged when passing through grain boundaries. However, independently of the pulse density, the samples with LSP evidence a decrease in the Cr content near the grain boundaries and an increase of the content of C and N in the grain boundary, Fig. 4 (b). This increase in the C and N content would be associated with the presence of carbides and nitrides. In ferritic stainless steels, intergranular corrosion is usually the result of the precipitation

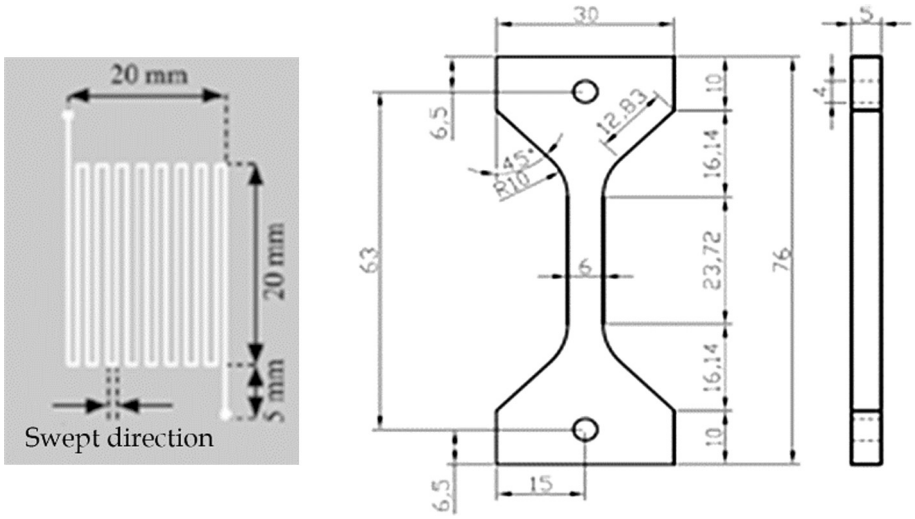

Fig. 1. Geometry of the fatigue specimens and schematic view of LSP processing.

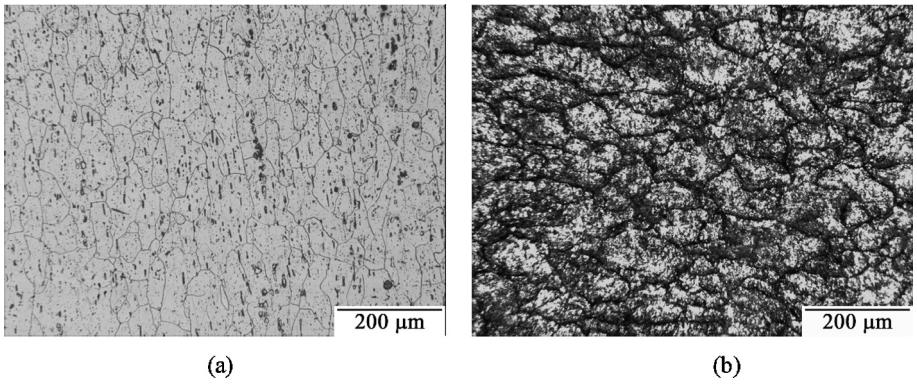

Fig. 2. Optical micrographs of the surface of UNS 44600 (a) without LSP etched by acid solution; (b) with LSP.

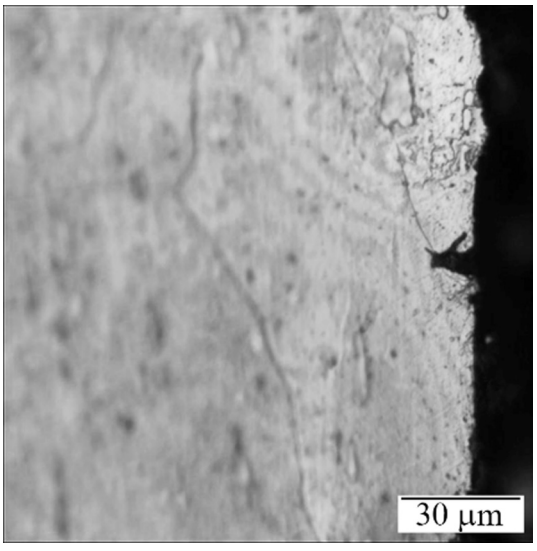

Fig. 3. Microstructure of the specimen cross section in UNS S44600 treated with LSP.

of $Cr_{23}C_6$ and Cr_2N in the grain boundaries that leads to a depletion of chromium in the vicinity of the grain boundary. This condition is called sensitization [29–31]. This phenomenon is more rapidly and at lower temperatures than in austenitic stainless steels due to the low solid solubility of C and N in ferritic stainless steels. Thus, when ferritic stainless steels, with interstitial content (C + N) greater than 0.03 wt.%, are heated to temperatures above 900 °C and then cooled, even as fast as water quenched, sensitization can occur [29]. When the steel is exposed to a corrosive environment, the area with Cr depletion causes intergranular corrosion. Considering the typical time frame of the peening experiments (Table 1), it is naturally expected that in a thin layer of present steel, LSPwC cause sensitization and subsequent intergranular corrosion under the confining water medium. Fig. 4(b) also revealed an increase of the oxygen content in certain zones of the LSP samples. Some authors indicate that as result of LSPwC an oxide layer and a melted and resolidified layer are found [11,16]. These thin surfaces layer are not uniform as the oxide layer can be removed during the plasma propagation in certain zones. This result agrees with the occurrence of a not uniform oxide layer caused by LSPwC in this steel.

Fig. 5 shows TEM micrographs of the near-surface microstructure in the AR and laser-shock peened states. The AR steel exhibits a low dislocation density, Fig. 5(a). On the other hand, a dense dislocation arrangements highly tangled is observed in laser shock peened samples, Fig. 5(b)–(d). It is inferred from these figures that the increase in the pulse density produces a higher dislocation density in the near surface region.

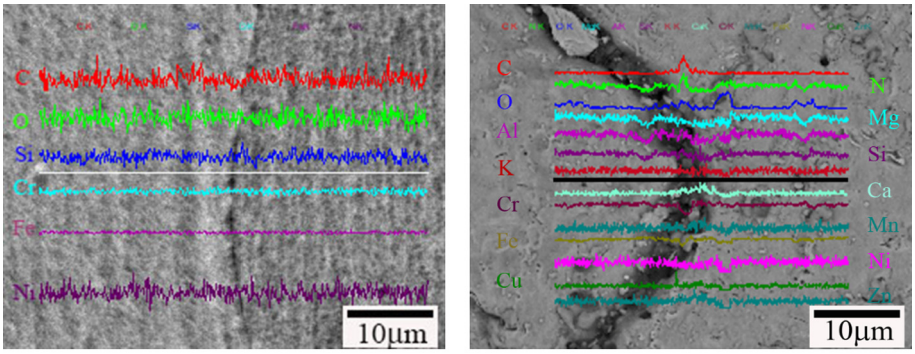

(a) (b)

Fig. 4. SEM with EDS along the grain boundary in UNS S44600 (a) AR and (b) treated with LSP.

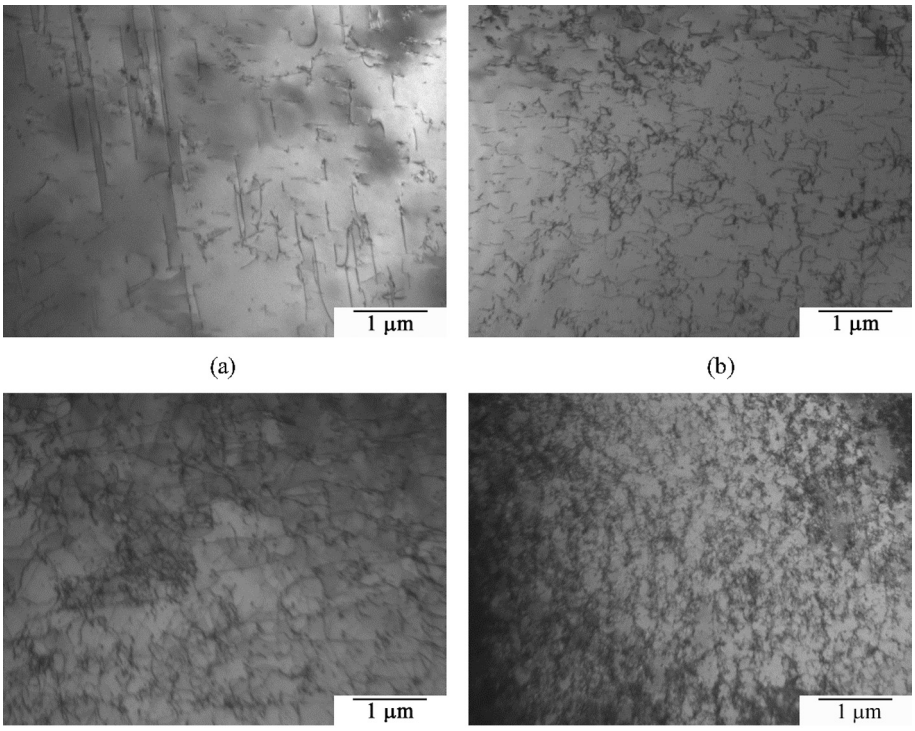

(a) (b)

(c) (d)

Fig. 5. Near-surface dislocation microstructure of UNS S44600 (a) AR and (b) LSP 1600 pulses/cm^2, (c) LSP 2500 pulses/cm^2 (d). LSP 5000 pulses/cm^2.

3.2. Hardening

The micro-hardness profiles over the specimen cross-section are displayed in Fig. 6. It is evident from this figure that LSP increases the surface hardness of the irradiated area (approx. 20–30%). This fact is consistent with the high dislocation density found in the near surface with LSP, Fig. 5(b) –(d). Moreover, it is important to note that a deepest penetration and a highest hardness is achieved by LSP at 5000 pulses/cm^2. In this sense, several authors claimed that hardness enhancement depends on the parameters selected for LSP treatment (substrate conditions, power density, peak pressure and number of impacts, etc) and alloy type [8,9].

3.3. Surface roughness

Table 2 shows the average roughness for the different pulse densities used in this work. It turned out that LPwC induced an increase in roughness with respect to the smooth surface of the unpeened samples. As the LSPwC can produce ablation and melting is expected that the surface roughness increase after this treatment [11–12,14–17]. Moreover, in the present work the roughness depend on the pulse density applied, larger roughness for higher pulse density. The above result are in line with those claimed by other authors [14,15,17].

3.4. Residual stresses

Residual stresses measurements as a function of depth, performed by the hole drilling method, are depicted in Fig. 7. Similar behavior is observed in the stress components parallel and perpendicular to the LSP scan direction. Therefore, in order to simplify the graphs only one curve for each pulse density is displayed. For the AR steel, the residual stress distribution takes a constant value of approximately −40 MPa. On the other hand, for all the studied

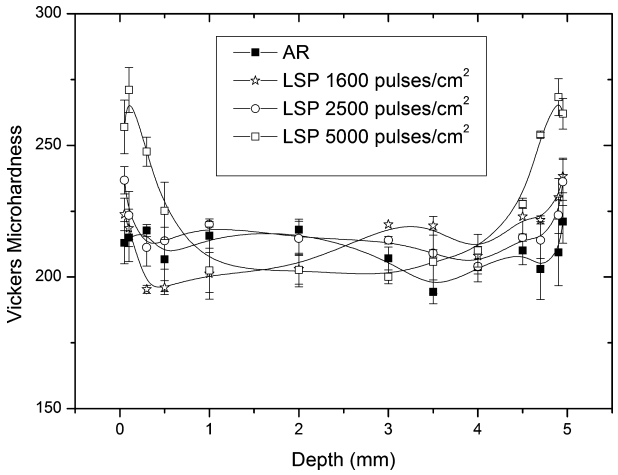

Fig. 6. Micro-hardness profiles across the specimen cross-section.

Table 2
R_a (average roughness).

Specimen	R_a (μm)
AR	0.40 ± 0.04
1600 pulses/cm^2	0.87 ± 0.06
2500 pulses/cm^2	1.13 ± 0.06
5000 pulses/cm^2	2.83 ± 0.20

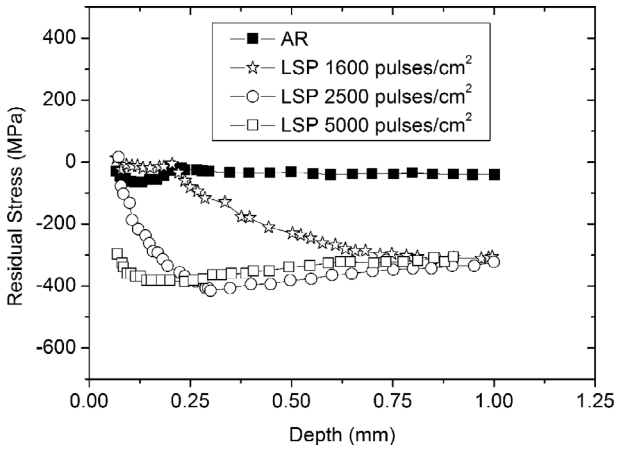

Fig. 7. Residual stress distribution on UNS S44600 specimens measured by hole-drilling.

pulse densities, the residual compressive stresses of treated samples reach an approximately constant value of −300 MPa. However, as the pulse density increases this value is reached nearer to the surface. Particularly with 5000 pulses/cm^2, the LSP induces this residual compression stress from 0.01 mm beneath the surface.

3.5. Fatigue performance

Fig. 8 shows the effect of LSP for the present steel on the low cycle fatigue behavior with two different plastic strain ranges. At $\Delta\varepsilon_p = 0.3\%$, Fig. 8(a), regardless of the pulse density, the LSP slightly raises the stress level and deteriorates the fatigue properties of this steel. It worthwhile to remark that the detriment in fatigue life is similar independently of the roughness induced by the LSPwC. Therefore, it can be speculated that though the roughness is an important factor that can deteriorate the fatigue properties, in this case is not the main responsible for such decrease in fatigue life.

During cyclic deformation, with increasing the applied stress amplitude, relaxation of induced residual stresses can occur [7,21–23]. Therefore, in order to reduce this phenomenon cyclic tests with lower plastic strain range were performed. Nevertheless, even at a lower strain range ($\Delta\varepsilon_p = 0.1\%$) the LSP has not improved the fatigue life of this steel, Fig. 8(b). At this strain range, also a similar fatigue life independently of the pulse density is observed. This fact provide a further proof of the not preponderant role of roughness.

The stability of the near surface microstructure is considered decisive to evaluate the usefulness of a mechanical surface treatment [7,22,32,33]. In this sense, investigations on shot peened SAE 1045 [33] showed that the relaxation of initial compressive residual stress is closely associated with microstructural alterations in the near surface regions during LCF tests. These researchers found the rearrangement of the high density of tangled dislocations into cells structures during cycling that leads to cyclic softening and a consequent relaxation of the original residual stresses induced by shot peening. They also observed that after identical fatigue conditions cell structures is the typical dislocation arrangement observed in near surface regions of shot peened and non-peened specimens. This result indicates that a completely relaxation of the residual stress induced by shot peening occurred.

It is well known that higher penetration depth of work hardening and compression residual stress leads to longer fatigue lifetime [7,8]. In this work, high penetration depth of work hardening and compressive residual were achieved with 5000 pulses/cm^2. Thus, this pulse density was selected to analyze the stability of the near surface dislocation structure during fatigue. Fig. 9 compares, beneath the surface, the dislocation arrangements of LSP with 5000 pulses/cm^2 and AR specimens cyclic tested at $\Delta\varepsilon_p = 0.3\%$ up to failure. From this figure, no evidence of discernible substructural difference is observed in the steel with and without LSP. In both cases, dislocation veins constitute the characteristic structure. It is inferred that, at this plastic strain range, not only the dislocation structure induced by LSP, Fig. 5(d), is not stable during cycling, Fig. 9(b), but also it achieves a similar dislocation configuration as the AR samples, Fig. 9(a). Nevertheless, the above results do not explain the detriment in fatigue life observed in LSP samples in comparison with the AR ones, Fig. 8(a). At least, if relaxation of residual stress induced by LSP occurs, a similar fatigue life in comparison with AR samples should be observed. During cycling at $\Delta\varepsilon_p = 0.1\%$, bundles of dislocations develop in the AR samples, Fig. 10(a), whereas the dislocation structure induced by LSP remains stable, Figs. 5(d) and 10(b). Hence, it can be presumed that for cyclic tests at low plastic strain range no relaxation of the residual stress induced by LSP occurs. However, an improvement of the fatigue life is not found even in this condition. Then, it is demonstrated that in the present steel the effect of LSP on the fatigue behavior is more complex than the single study of residual compression stress induced by it. The thermal effects caused by the LSP, without protective coating, in UNS S44600, with interstitial content greater than 0.03 wt.%, exposed to the corrosive medium as water should not be overlooked. Owing to this process, well known as sensitization, intergranular corrosion was previously observed, Fig. 4(b). As result of this intergranular corrosion, independently of the strain range applied, cracks nucleate in grain boundaries during fatigue, Fig. 11(a). Yan et al. [34] found a chromium depletion area along the grain boundary in aged HR3Calloy. They reported that during a tensile test at room temperature, this chromium depleted zones encourage the crack nucleation at the carbide-matrix interface when the stress concentration is sufficient high. On the other hand, Akita et al. [35] studied the effects of heat treatment on the fatigue behaviur of a superferritic stainless steel,

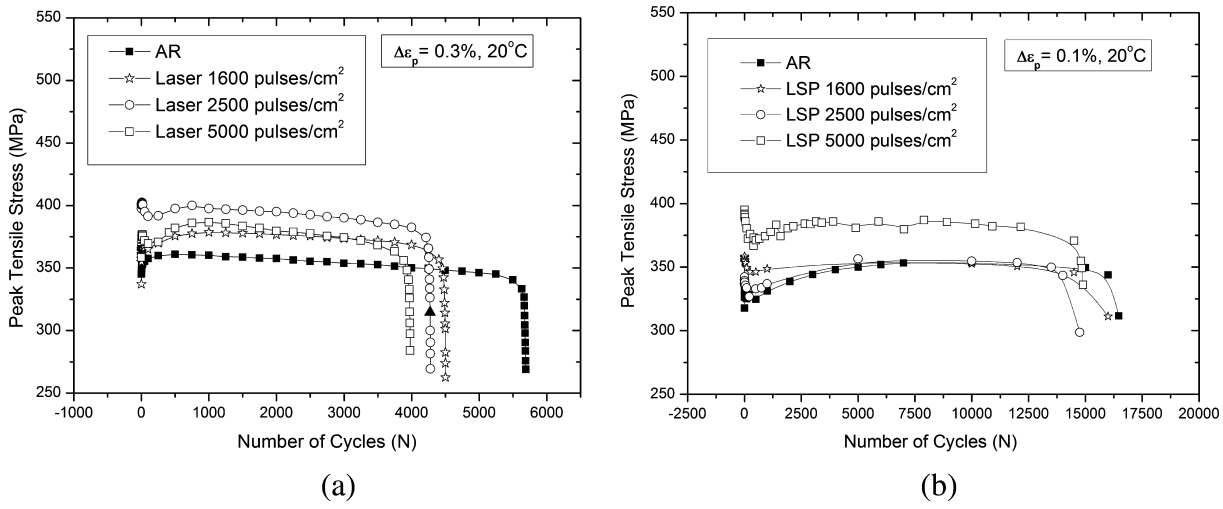

Fig. 8. Cyclic deformation curves of UNS S44600 for different LSP conditions and plastic strain ranges.

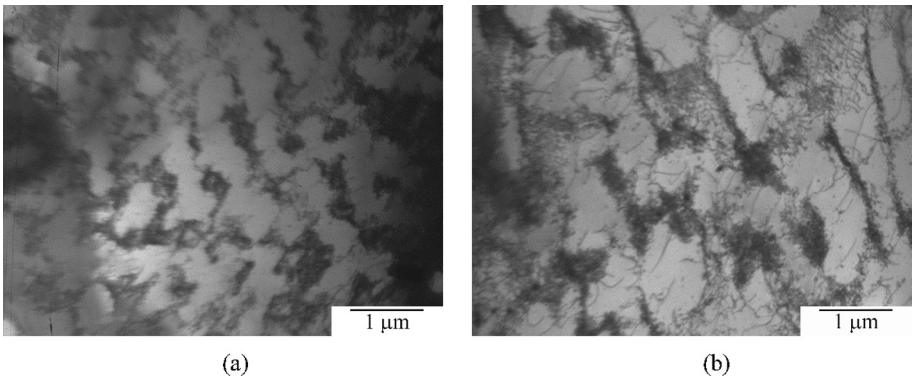

Fig. 9. Bright field TEM images of the near surface microstructure of UNS S44600 cyclic tested at $\Delta\varepsilon_p = 0.3\%$ to fracture (a) AR and (b) LSP 5000 pulses/cm^2.

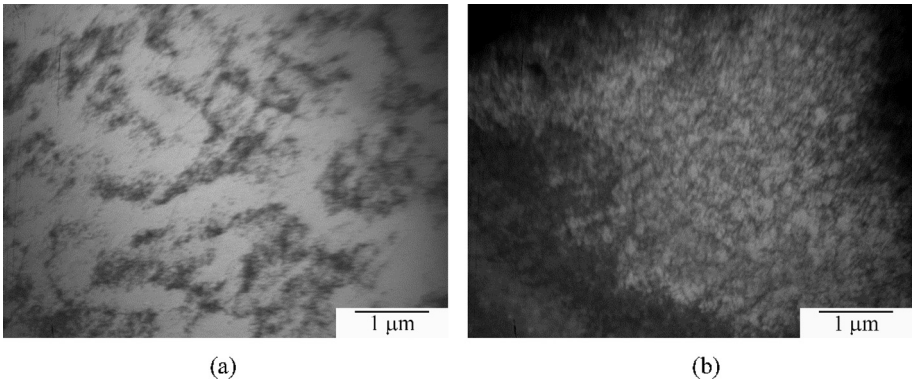

Fig. 10. Bright field TEM images of the near surface microstructure of UNS S44600 cyclic tested at $\Delta\varepsilon_p = 0.1\%$ to failure (a) AR and (b) LSP 5000 pulses/cm^2.

type 444. These authors believe that in the water-quenched condition, the induced chromium-depleted zones along the grain boundaries would be responsible for the decrease of fatigue strength and the origin of grain boundary crack nucleation. Thus, the surface irregularities caused by intergranular corrosion observed in this work could act as stress intensifier, leading to crack nucleation in zone where the stress concentration is relatively larger than other regions. This assumption is consistent what it is proposed by other authors [34,35]. On the contrary, cracks initiate and grow along extrusions within the grains in fatigued AR specimen, Fig. 11(b). Thus, in the present steel at $\Delta\varepsilon_p = 0.1\%$, the advantage of the negligible relaxation of the induced compressive residual stresses have the counterbalance of the intergranular corrosion damage caused by the LSP without coating. The similar fatigue life observed between AR and LSP specimens is consistent with this assumption, Fig. 8(b). On the other hand, at $\Delta\varepsilon_p = 0.3\%$ the relaxation of the induced residual stress cannot compensate the detrimental effect of intergranular corrosion, Fig. 8(a).

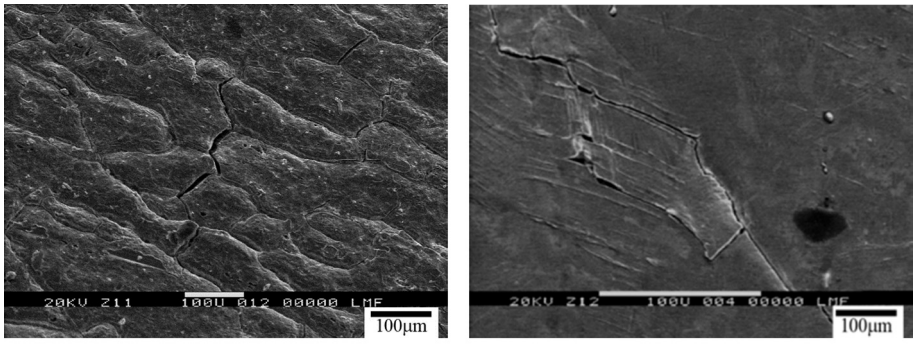

Fig. 11. SEM images of the fatigued surface of UNS S44600 (a) LSP at 5000 pulses/cm^2 and (b) AR.

4. Conclusions

This investigation aims to addressing the effect of LSP, without protective overlay and with different pulse densities, on low cycle fatigue behaviur of UNS S44600 ferritic stainless steel. The main conclusions resulting from the study can be summarized as follows:

(i) The laser shock peening microstructure is characterized by intergranular corrosion, within the 10 µm beneath the surface, and an increase in dislocation density in the near surface regions.
(ii) At the surface, the hardness and roughness of the LSP condition is higher than that of AR condition. A deepest penetration and a highest hardness is achieved by LSP at 5000 pulses/cm^2 whereas a higher roughness is obtained with an increase in pulse density.
(iii) Independently of the pulse density, the maximum residual compressive stress induced by LSP is approximately −300 MPa. However, as the pulse density increases this value is reached nearer to the surface.
(iv) At high plastic strain ranges, the LSP deteriorates the fatigue properties. The relaxation of the residual stress induced by LSP cannot counterbalance the detrimental effect of the intergranular corrosion caused by the process.
(v) At low plastic strain ranges, the advantages of the induced residual stress compensate the effects of the intergranular corrosion.
(vi) At high and low plastic strain ranges, the roughness induced by LSPwC is not the main responsible for the decrease in fatigue life.
(vii) The LSP is not effective in improving the low cycle fatigue behavior of this steel. Though LSPwC produces beneficial compression residual stresses it also causes intergranular corrosion that deteriorates fatigue life.

Acknowledgements

This work was supported by Agencia Nacional de Promoción Científica y Tecnológica (PICT-2013-1105) and by the Cooperation Program Conacyt/Mincyt (MX/11/12) between México and Argentina.

References

[1] J.C. Stinville, P. Villechaise, C. Templier, J.P. Riviere, M. Drouet, Plasma nitriding of 316L austenitic stainless steel: Experimental investigation of fatigue life and surface evolution, Surface and Coatings Technology 204 (2010) 1947–1951.
[2] H. Kovaci, A.F. Yetim, Ö. Baran, A. Çelik, Fatigue crack growth analysis of plasma nitrided AISI 4140 low-alloy steel: Part 1-constant amplitude loading, Materials Science & Engineering A 672 (2016) 257–264.
[3] S.P. Brühl, A. Cabo, W. Tuckart, G. Prieto, Tribological behaviour of nitrided and nitrocarburized carbon steel used to produce engine parts, Industrial Lubrication and Tribology 68 (1) (2016) 125–133.
[4] I. Yegen, M. Usta, The effect of salt bath cementation on mechanical behavior of hot-rolled and cold-drawn SAE 8620 and 16MnCr5 steels, Vacuum 85 (2010) 390–396.
[5] V. Llaneza, F.J. Belzunce, Study of the effects produced by shot peening on the surface of quenched and tempered steels: roughness, residual stresses and work hardening, Applied Surface Science 356 (2015) 475–485.
[6] S. Bagherifard, I. Fernandez-Pariente, R. Ghelichi, M. Guagliano, Effect of severe shot peening on microstructure and fatigue strength of cast iron, International Journal of Fatigue 65 (2014) 64–70.
[7] V. Schulze, *Modern Mechanical Surface Treatment, states, stability, effects*, Wiley-Vch, 2006.
[8] C.S. Montross, T. Wei, L. Ye, G. Clark, Y.-W. Mai, Laser shock processing and its effects on microstructure and properties of metal alloys: a review, International Journal of Fatigue 24 (2002) 1021–1036.
[9] A.K. Gujba, M. Medraj, Laser Peening Process and Its Impact on Materials Properties in Comparison with Shot Peening and Ultrasonic Impact Peening, Materials 7 (2014) 7925–7974, doi:10.3390 /ma7127925.
[10] Y.Y. Xu, X. Dong Ren, Y.K. Zhang, J.Z. Zhou, X. Q. Zhang. Coating Influence on Residual Stress in Laser Shock Processing, Key Engineering Materials 353–358 (2007) 1753–1756.
[11] A.S. Gill, A. Telang, V.K. Vasudevan, Characteristics of surface layers formed on Inconel 718 by laser shock peening with and without a protective coating, Journal of Materials Processing Technology 225 (2015) 463–472.
[12] D. Karthik, S. Swaroop. Laser Peening Without Coating - an Advanced Surface Treatment: A Review. Materials and Manufacturing Processes 2016. Accepted paper. doi/full/10.1080/10426914.2016.1221095.
[13] Y. Sano, K. Akita, K. Masaki, Y. Ochi, I. Altenberger, B. Scholtes, Laser Peening without Coating as a Surface Enhancement Technology, JLMN-Journal of Laser Micro/Nanoengineering 1 (3) (2006) 161–166.
[14] D. Karthik, S. Kalainathan, S. Swaroop, Surface modification of 17–4 PH stainless steel by laser peening without protective coating process, Surface & Coatings Technology 278 (2015) 138–145.
[15] D. Karthik, S. Swaroop, Laser peening without coating induced phase transformation and thermal relaxation of residual stresses in AISI 321 steel, Surface & Coatings Technology 291 (2016) 161–171.
[16] Y. Sano, M. Obata, T. Kubo, N. Mukai, M. Yoda, K. Masaki, Y. Ochi, Retardation of crack initiation and growth in austenitic stainless steels by laser peening without protective coating, Materials Science and Engineering: A 417 (1–2) (2006) 334–340.
[17] S. Kalainathann, S. Sathyajith, S. Swaroop, Effect of laser shot peening without coating on the surface properties and corrosion behavior of 316L steels, Optics and Lasers in Engineering 50 (2012) 1740–1745.
[18] N.F. Ren, H.M. Yang, S.Q. Yuan, Y. Wang, S.X. Tang, L.M. Zheng, X.D. Ren, F.Z. Dai, High temperature mechanical properties and surface fatigue behavior improving of steel alloy via laser shock peening, Materials and Design 53 (2014) 452–456.
[19] S. Huang, J.Z. Zhou, J. Sheng, K.Y. Luo, J.Z. Lu, Z.C. Xu, X.K. Meng, L. Dai, L.D. Zuo, H.Y. Ruan, H.S. Chen, Effects of laser peening with different coverage areas on fatigue crack growth properties of 6061–T6 aluminum alloy, International Journal of Fatigue 47 (2013) 292–299.
[20] X. Chen, J. Wang, Y. Fang, B. Madigan, G. Xu, J. Zhou, Investigation of microstructures and residual stresses in laser peened Incoloy 800H weldments, Optics & Laser Technology 57 (2014) 159–164.
[21] C. Rubio-González, A. Garnica - Guzmán, G. Gómez-Rosas, Relaxation of residual stresses induced by laser shock processing, Revista Mexicana de física 55 (4) (2009) 256–261.
[22] C. Ye, S. Suslov, B.J. Kim, E.A. Stach, G.J. Cheng, Fatigue performance improvement in AISI 4140 steel by dynamic strain aging and dynamic

precipitation during warm laser shock peening, Acta Materialia 59 (2011) 1014–1025.
[23] I. Nikitin, I. Altenberger, Comparison of the fatigue behavior and residual stress stability of laser-shock peened and deep rolled austenitic stainless steel AISI 304 in the temperature range 25–600°C, Materials Science & Engineering A 465 (1–2) (2007) 176–182.
[24] C. Correa, L. Ruiz de Lara, M. Díaz, A. Gil-Santos, J.A. Porro, J.L. Ocaña, Effect of advancing direction on fatigue life of 316L stainless steel specimens treated by double-sided laser shock peening, International Journal of Fatigue 79 (2015) 1–9.
[25] C. Rubio-González, C. Felix - Martinez, G. Gomez-Rosas, J.L. Ocaña, M. Morales, J.A. Porro, Effect of laser shock processing on fatigue crack growth of duplex stainless steel, Materials Science & Engineering A 528 (2011) 914–919.
[26] D. Janikowski, W. Henricks, Superferritic Stainless Steels-The Cost Effective Answer for Heat Transfer Tubing REF: MP07-016, World Congress on Desalination and Water Reuse, Gran Canaria, Spain, 2007.
[27] Standard Test Method for Determining Residual Stresses by the Hole-drilling Strain Gage Method, Annual Book of ASTM Standards, v. 03.01, No. E837–01, ASTM, 2002.
[28] L. Zhou, W. He, S. Luo, C. Long, C. Wang, X. Nie, G. He, X. Shen, Y. Li, Laser shock peening induced surface nanocrystallization and martensite transformation in austenitic stainless steel, Journal of Alloys and Compounds 655 (2016) 66–70.
[29] D.T. Llewellyn, R.C. Hudd. Steels: Metallurgy and Applications 1998. Third Edition.
[30] K. Nilsson. *Corrosion tests of stainless steels in automotive applications.* Master's thesis 2006. Lulea University of Technology. http://epubl.ltu.se/1402-1617/2006/089/LTU-EX-06089-SE.pdf.
[31] B. Leffler, STAINLESS- stainless steels and their properties, Avesta, Sweden, 1998, http://www.improve.it/metro/file.php?file=/1/Papers/Metallurgy_of_Welding_Processes/STAINLESS_.pdf.
[32] I. Altenberger, B. Scholtes, U. Martin, H. Oettel, Cyclic deformation and near surface microstructures of shot peened or deep rolled austenitic stainless steel AISI 304, Materials Science & Engineering A 264 (1999) 1–16.
[33] U. Martin, I. Altenberger, B. Scholtes, K. Kremmer, H. Oettel, Cyclic deformation and near surface microstructures of normalized shot peened steel SAE 1045, Materials Science & Engineering A 246 (1998) 69–80.
[34] J. Yan, Y. Gu, F. Sun, Y. Xu, Y. Yuan, J. Lu, Z. Yang, Y. Dang, Evolution of microstructure and mechanical properties of a 25Cr-20Ni heat resistant alloy after long-term service, Materials Science & Engineering A 675 (2016) 289–298.
[35] M. Akita, M. Nakajima, Y. Uematsu, K. Tokaji, Effects of annealing and quenching on fatigue behaviour in type 444 ferritic stainless steel, Fatigue & Fracture of Engineering Materials & Structures 31 (2008) 959–966.